

CFD SIMULATIONS OF MULTI-DIRECTIONAL IRREGULAR WAVE INTERACTION WITH A LARGE CYLINDER

Weizhi Wang*

Department of Civil and Environmental Engineering
Norwegian University of Science and Technology
Trondheim 7491, Norway
Email: weizhi.wang@ntnu.no

**Arun Kamath
Hans Bihs**

Department of Civil and Environmental Engineering
Norwegian University of Science and Technology
Trondheim 7491, Norway

ABSTRACT

Ocean waves are random by nature and can be regarded as a superposition of a finite number of regular waves traveling in different directions with different frequencies and phases. Cylinder-shaped objects are commonly present in most coastal structures. An irregular bottom topography has a significant influence on the wave behaviours and therefore the wave forces on the coastal structures. A numerical approach that is able to calculate the wave forces on a cylinder in a multi-directional irregular wave field over an irregular bottom is desired. As Computational Fluid Dynamics (CFD) is able to represent most of the wave behaviour with few assumptions, it is considered to be an attractive option to address these issues. The open-source CFD wave model REEF3D has shown good performances in simulating wave propagation over irregular bottoms and a good prediction of wave forces on a cylinder in a uni-directional wave field, yet the ability to calculate the wave force in a multi-directional irregular sea needs to be validated. Therefore, this paper attempts to simulate the multi-directional random sea interaction with a large cylinder using REEF3D and validate the results. A novel approach of multi-directional irregular wave generation method in a CFD-based numerical wave tank is introduced. Only even-bottom tanks are considered in this study, leaving the irregular bottom simulation for future studies. Furthermore, among many factors that influence the wave forces, this paper focuses particularly on the effect of the wave steepness. The effects of wave steepness in regular waves, uni-directional irregular waves and multi-directional irregular waves are investigated. Goda's

JONSWAP frequency spectrum and the frequency-independent Mitsuyasu directional spreading function are used to generate the multi-directional irregular waves. The wave forces due to the multi-directional irregular waves in the numerical tank are compared with experimental data. The performance of the CFD simulation is analysed and discussed.

INTRODUCTION

The coastal region is highly populated and hosts several social and economic activities. A continuously increasing number of coastal structures are being constructed in the coastal waters. These coastal structures are subject to complex wave impacts, and the wave forces on the structures are of critical concern for engineering design and safety. Most coastal structures consist of a large amount of cylinder-shape components. Therefore, the study of wave forces on cylinders is a topic of great interest for coastal engineers. For most slender cylinders, with the cylinder diameter to wavelength ratio smaller than 0.15 ($D/L \leq 0.15$) [1], the Morison equations [2] are valid and widely used. However, when the diameter to wavelength ratio becomes larger, the diffraction of waves becomes dominant, in which case the diffraction theory needs to be applied for force calculation. MacCamy [3] developed a linear diffraction theory which can be successfully applied for waves with relatively small steepness. For waves with higher steepness, non-linear effects become more important, which requires higher-order diffraction theories. Kriebel et al. [4] [5] and Newman et al. [6] have explored several high-order diffraction theories and achieved better results than

*Address all correspondence to this author.

linear theory in non-linear wave fields. Wang et al. [7] and Morgan et al. [8] also carried out numerical studies on the non-linear wave-cylinder interaction using the computational fluid dynamics (CFD) method and achieved good agreements with the experimental data.

Most of the studies are performed with uni-directional waves, and there are few studies carried out with multi-directional irregular waves. Due to the complicated topography and local wind conditions, the coastal waves are composed of short-crested multi-directional irregular waves. Wave forces on cylinders in short-crested waves is an ongoing challenge. Ji et al. [1] carried out a series of experiments on the wave force on a large cylinder in a multi-directional irregular wave field. Li et al. [9] [10] also performed a series of experimental studies of 3D focused wave incident on a cylinder. However, there are few numerical simulations to calculate wave forces due to multi-directional irregular waves on a large cylinder. Numerical models such as HOS-NWT [11] and HOS-Ocean [12] were developed at Ecole Centrale de Nantes for multi-directional irregular wave simulation in a wave basin. Compared to a wave basin, the real coastal region has more complicated sea-bed topography and irregular boundaries. A numerical model that can not only simulate the multi-directional irregular wave but is also able to investigate the wave propagation over complicated bottom boundaries is needed for more universal applications.

One solution to the complexity presented in the coastal region is to deploy the CFD method. Paulsen et al. [13] proposed a domain decomposition method to combine a fully-nonlinear potential flow solver with a CFD solver to study the multi-directional irregular wave impact on a vertical cylinder. The wavemaker kinematics at the wave gauges in the experiment were reconstructed as inputs in the potential flow model. Then the waves generated from the potential flow model are used as boundary condition for the CFD model. However, this method limits the application of their model when the experimental data is not available and also limits what kind of wave can be generated. Using a directional spectrum to generate waves will give a significant flexibility to generate any types of waves following various spectra. Further, it is not a wave generation implementation for a CFD-based model in the work of Paulsen et al. [13]. A direct wave generation using CFD has not been investigated. In this paper, a novel approach for multi-directional irregular wave generation in a CFD-based numerical wave tank is investigated using the wave model REEF3D.

REEF3D is an open-source CFD wave model developed at NTNU with a focus on wave hydrodynamics and coastal and marine applications. Its wide application on various complex free-surface flow makes it an attractive alternative for multi-directional irregular wave generation using a wave spectrum.

Several numerical studies on wave-cylinder interaction have been performed using REEF3D. Bihs et al. [14] numerically investigated the focused wave interaction with a vertical cylinder. Kamath et al. [15] [16] studied the interaction between regular waves and cylinder arrays. Alagan Chella et al. [17] also studied the breaking wave interaction with a bottom mounted slender cylinder. REEF3D has also been successfully used to address various other challenges. For example, Grotle et al. [18] used REEF3D to model the sloshing under roll excitation, Bihs and Kamath [19] performed simulations of a 6 DOF floating body using REEF3D with a combined level-set and ghost cell immersed boundary method. Wang et al. [20] [21] also successfully used REEF3D to simulate the wave propagation over natural topographies in the Norwegian fjords and harbours. REEF3D provides a high-resolution free-surface and predicts the wave interaction with structures in an accurate and reliable manner. A multi-directional irregular wave module is implemented in the REEF3D framework and is used in the current study. The multi-directional irregular wave fields are generated directly using the directional spectrum in REEF3D.

Using the new CFD wave generation method for multi-directional irregular waves, the wave forces on a vertical cylinder with different wave steepnesses are studied in this paper. First, regular waves and uni-directional irregular waves are simulated to provide a fundamental understanding of the influence of wave steepness on the wave forces. Next, multi-directional irregular wave forces are calculated from the numerical wave tank and the results are compared to the measurements in the experiment [1]. The simulation shows a similar relation between wave force and wave steepness as in the experiment. However, there are differences in wave force changing rate and the values of the forces. The differences between the numerical results and the experimental measurements are analysed. The effect of irregularity is also discussed. Some intriguing topics that arise from the current work are also discussed as future work. The multi-directional irregular wave propagation over irregular bottom is not included in this paper but will be investigated in the future research.

NUMERICAL MODEL

The Governing Equations

REEF3D solves the three-dimensional incompressible Navier-Stokes equation together with the continuity equation as shown in Eqn. (1) and Eqn. (2).

$$\frac{\partial u_i}{\partial x_i} = 0 \quad (1)$$

$$\frac{\partial u_i}{\partial t} + u_j \frac{\partial u_i}{\partial x_j} = -\frac{1}{\rho} \frac{\partial p}{\partial x_i} + \frac{\partial}{\partial x_j} \left[\nu \left(\frac{\partial u_i}{\partial x_j} + \frac{\partial u_j}{\partial x_i} \right) \right] + g_i \quad (2)$$

where u is the velocity, ρ stands for the fluid density, p represents the pressure, ν is the kinematic viscosity and g is the acceleration due to gravity.

A finite difference method is applied to solve the governing equations on a structured staggered Cartesian grid. A conservative fifth-order weighted essentially non-oscillatory (WENO) scheme [22] and a third-order Total-Variation-Diminishing (TVD) Runge-Kutta scheme [23] are used. The high-order numerical schemes assure high accuracy of the numerical results. The PFMG preconditioned BiCGStab algorithm provided by the HYPRE library [24] is used to solve the Poisson equation.

The Free-surface Modelling

The level-set method is used for the free surface capturing. Acting as a signed distance function, the level-set function $\phi(\vec{x}, t)$ equals to zero at the phase interface and shows opposite signs in the two different phases, as shown in Eqn. (3) [25].

$$\phi(\vec{x}, t) \begin{cases} > 0 \text{ if } \vec{x} \in \text{phase 1} \\ = 0 \text{ if } \vec{x} \in \Gamma \\ < 0 \text{ if } \vec{x} \in \text{phase 2} \end{cases} \quad (3)$$

The waves are generated and absorbed at the wave generation zone and the numerical beaches using the relaxation method [26]. The relaxation function proposed by Jacobsen [27] is used in the code, as shown in Eqn. (4). In the wave generation zone, the free-surface elevation, velocity and pressure are ramped up to the designed theoretical values. At the numerical beach, the velocities are decreased gradually to zero, the free-surface and the pressure are restored to the still water level and the hydrostatic pressure respectively.

$$\Gamma(\tilde{x}) = 1 - \frac{e^{(\tilde{x}^{3.5})} - 1}{e - 1} \text{ for } \tilde{x} \in [0; 1] \quad (4)$$

where \tilde{x} is scaled to the length of the relaxation zone.

The Multi-directional Irregular Wave Generation in a Numerical Tank

The method of superposition is used to construct 3D irregular waves from a finite number of regular wave components

with different directions, frequencies and phases. The relaxation method is used to generate the waves in the numerical wave tank. The surface elevation, velocity and pressure are ramped up to the designed theoretical values in the wave generation relaxation zone. The theoretical values are calculated from the directional spectrum. A directional spectrum is formed by multiplying a power spectrum and a directional spreading function. The JONSWAP spectrum recommended by Goda [28], as shown in Eqn. (5), is used in this paper as the power spectrum.

$$S(f) = \beta_J H_s^2 T_p^{-4} f^{-5} \exp(-1.25(T_p f)^{-4}) \gamma^{\exp(-\frac{(T_p f - 1)^2}{2\sigma^2})} \quad (5)$$

in which,

$$\beta_J = \frac{0.06238}{0.230 + 0.0336\gamma - 0.185(1.9 + \gamma)^{-1}} (1.094 - 0.01915 \ln(\gamma)) \quad (6)$$

$$\sigma = \begin{cases} 0.07 & \text{if } \omega \leq \omega_p \\ 0.09 & \text{if } \omega \geq \omega_p \end{cases} \quad (7)$$

In the formula, H_s stands for significant wave height (m) and T_p stands for the peak period (s). The peak enhancement factor γ is typically chosen to be 3.3.

The frequency-independent Mitsuyasu directional spreading function is used in this paper. The Mitsuyasu function [29] is derived by fitting the directional data captured by a cloverleaf buoy. It introduces a single shape parameter s and multiplies a normalisation factor $G_0(s)$, as shown in Eqn. (8).

$$G(\beta) = G_0(s) \cos^{2s} \left(\frac{\beta}{2} \right) \quad (8)$$

where

$$G_0(s) = \frac{1}{\pi} 2^{(2s-1)} \frac{\Gamma^2(s+1)}{\Gamma(2s+1)} \quad (9)$$

In the function, Γ stands for the Gamma function. $\bar{\beta}$ is the principal direction representing the major energy propagation direction and β_i is the direction of each incident wave components measured from the principal direction counter-clockwise.

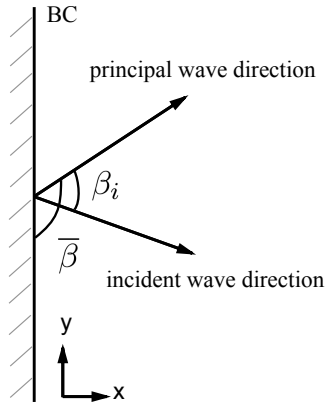


FIGURE 1. The definition of the principal angle and the incident wave angle

The angles as illustrated in Fig. 1. The shape parameter s in the formulas is not dependent on frequency and can be assigned manually.

By multiplying Eqn. (5) and Eqn. (8), the joint directional spectrum is obtained. The surface elevation is calculated with Eqn. (10). k_n is calculated based the corresponding wave theory and the wave amplitude is calculated with Eqn. (11) from the spectrum.

$$\eta(\vec{r}, t) = \sum_{i=1}^N a_n \cos(\vec{k}_n \cdot \vec{r} - \omega_n t + \varepsilon_n) \quad (10)$$

$$a_n = \sqrt{2S(\omega_n, \beta_n) \Delta\omega \Delta\beta} \quad (11)$$

where g is gravitational acceleration $9.81m/s^2$, θ_0 is the formulation derived by [30]. ε_n is the phase generated randomly between 0 and 2π .

To implement the wave generation in the code, a double summation method is used, meaning that waves at different frequencies travel in different directions, and waves at the same frequency travel in different directions too. The frequency and angular information are each stored in a single-array so that all the combinations of frequencies and angles are included and at the same time the computational complexity is reduced. N denotes the total number of the wave components, which is a product of the number of frequency components and direction components.

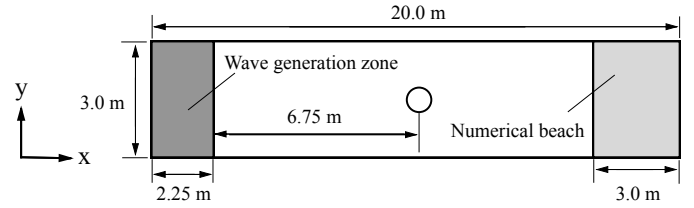


FIGURE 2. The configuration of the numerical wave tank for the uni-directional regular and irregular wave simulation

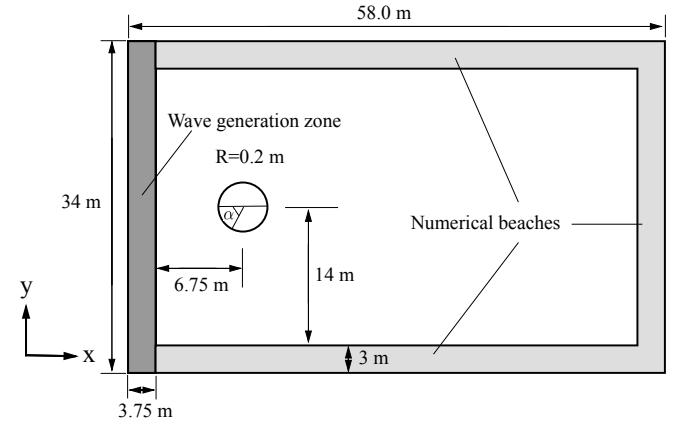


FIGURE 3. The configuration of the numerical wave tank for the multi-directional irregular wave simulation

Numerical Tank Configurations

For the uni-directional waves, the numerical tank is 20 m long and 3 m wide with a water depth of 0.7 m. The configuration of the numerical tank is illustrated in Fig. 2. For the multi-directional wave simulation, the numerical wave tank is chosen to be of the same size as in the experiment [1]. The tank is 58 m long, 34 m wide and 0.7 m deep. The configuration for the multi-directional wave tank is shown in Fig. 3. As can be seen, numerical beaches are arranged at the end of the tank as well as at the side walls. The vertical cylinder used in this study has a radius of 0.2 m and a height of 1.2 m. Following the setups in the experiment, the cylinder is located at 6.75 m from the wave generation zone and in the middle of the width. For the uni-directional irregular wave simulations, Goda's JONSWAP spectrum is used as the input spectrum. For the multi-directional irregular wave simulation, the combined JONSWAP-Mitsuyasu spectrum is adopted.

NUMERICAL RESULTS

The simulation results with different incident waves are presented in this section. The mesh convergence study is presented for both regular and irregular wave cases. The changes in the wave forces with wave steepness are then shown for each case.

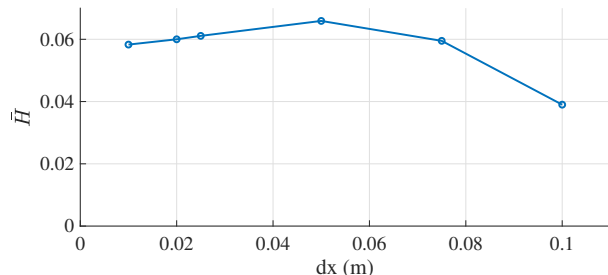


FIGURE 4. Variation of the mean wave heights in the numerical wave tank for different mesh sizes in the regular wave simulations

The comparison between the numerical results and the experimental data for the multi-directional irregular waves is also discussed.

Regular Wave Forces on a Large Cylinder

The input regular waves have the wave heights of 0.04 m, 0.06 m and 0.08 m and share the same wave period of 0.9 s. Three different waves with three different wave steepnesses are simulated. For the mesh convergence study, the mean wave heights for different mesh sizes during a 60 s simulation in a 2D tank are presented in Fig. 4. The wave forces convergence is also studied. The simulated forces are normalised for the convenience of comparison. The normalisation factor is shown in Eqn. (12), where r represents the radius of the cylinder. The normalised forces with different mesh sizes are shown in Fig. 5. It shows that the mesh size of 0.02 m gives a good agreement with the input wave and relatively converged force. Therefore the following wave force simulations are performed with the mesh size of 0.02 m. This results in about 7.5 million mesh cells. It takes about 6 hours to finish one simulation of 90 s with 512 processors. The normalised forces with different wave steepnesses from the numerical wave tank are shown in Fig. 6. It is seen that with increasing steepness, the wave force also increases accordingly. It also indicates the trend of increase is almost linear within the chosen steepness range.

$$F_{norm} = \rho g r^3 \quad (12)$$

Uni-directional Irregular Wave Forces on a Large Cylinder

Three waves with significant wave heights of 0.04 m, 0.06 m and 0.08 m with the same peak period of 0.9 s are simulated in this study. The numerical tank configurations are the same as for the regular wave simulation in the previous section. 200 frequencies are used for the irregular wave generation. All simulations

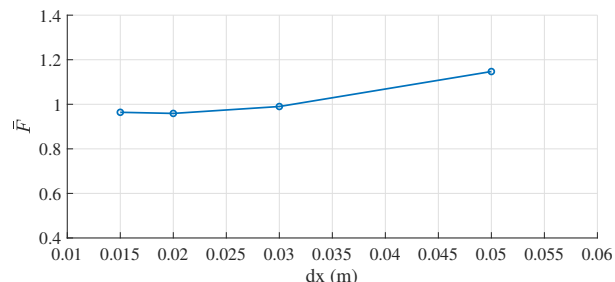


FIGURE 5. Variation of the normalised mean wave force in the numerical wave tank for different mesh sizes in the regular wave simulations

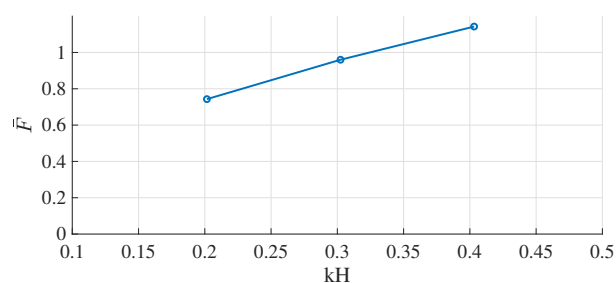


FIGURE 6. The normalised mean wave forces with different wave steepnesses in the regular wave simulations

last 300 s, allowing a sufficient time for all the wave components to pass the wave gauges, that is to get a complete wave spectrum in the numerical wave tank. Considering the irregularity of the wave field, an independent mesh convergence study is conducted in this section. Fig. 7 shows the power spectrum in the numerical tank for different meshes. At a mesh size of 0.015 m and 0.02 m, the power spectra almost match the theoretical input wave spectrum, with minor energy loss at the peak frequency. Fig. 8 plots the significant wave heights H_s with different meshes. It shows that, despite some energy loss, the value of the calculated H_s is not affected significantly. Similarly, the normalised forces at different meshes are shown in Fig. 9. The forces are also considered accurate enough at mesh size of 0.02 m. Considering both accuracy and computational efficiency, a mesh size of 0.02 m is considered to be adequate for the current application, resulting in about 7.5 million mesh cells in the numerical wave tank. For a 600 s simulation, it takes about 50 hours with 1024 cores on the supercomputer. The resulting normalised significant wave forces are plotted with regard to the wave steepness in Fig. 10. It shows a similar trend as the regular wave. At the same time, the wave force changes are slightly bigger among different steepnesses.

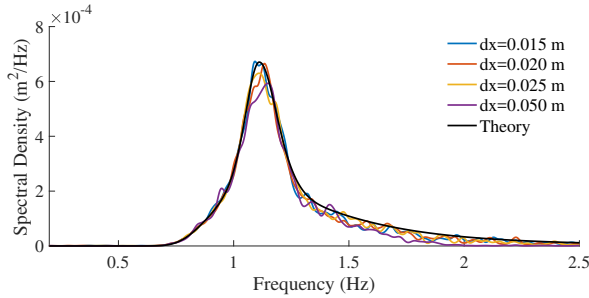


FIGURE 7. The power spectra in the numerical wave tank (without the cylinder) with different mesh sizes in the uni-directional irregular wave simulations at the location where the cylinder should be

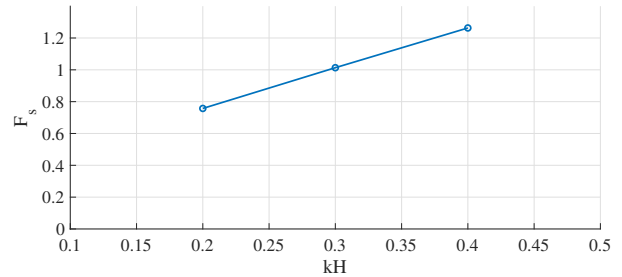


FIGURE 10. The normalised significant wave forces with different wave steepnesses in the uni-directional irregular wave simulations

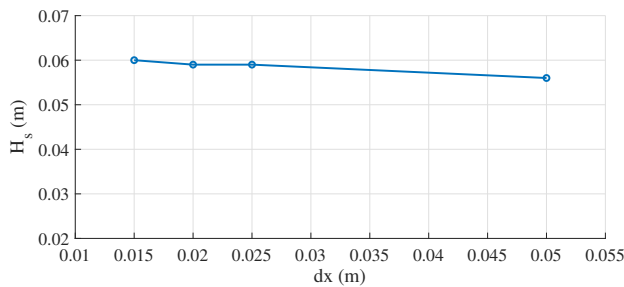


FIGURE 8. The significant wave height H_s in the numerical wave tank with different mesh sizes in the uni-directional irregular wave simulations

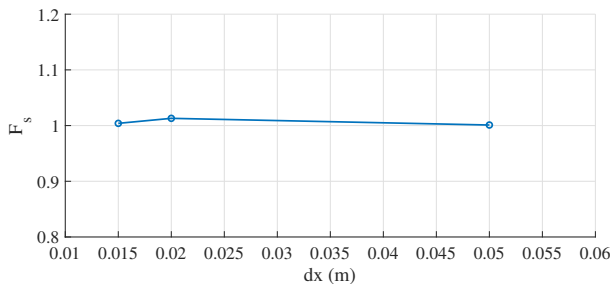


FIGURE 9. The normalised significant wave forces with different mesh sizes in the uni-directional irregular wave simulations

Multi-directional Irregular Wave Forces on a Large Cylinder

The numerical tank setups are described in Fig. 3. The multi-directional irregular wave generation benefits from the wide wave generation boundary. At the same time, the tank is long and wide enough to reduce reflection of waves from the boundaries of the tank. The cylinder is located very close to the wave generation boundary which keeps the disturbances in the wave propagation process to a minimum. The input

waves also have significant wave heights of 0.04 m, 0.06 m and 0.08 m, with a shared peak period of 0.9 s. The numerical setups closely follow the experiment [1]. The principal direction is 0° and the shape parameter s in Eqn. (8) is set to be 20, which corresponds to a narrow bandwidth spreading. A JONSWAP power spectrum and a frequency-independent Mitsuyasu spreading function are adopted. The power spectrum, directional spreading function and the directional spectrum corresponding to the wave condition with $H_s = 0.06m$ and $T_p = 0.9s$ are shown in Fig. 11, Fig. 12 and Fig. 13. For the wave generation, 50 frequency components and 6 directional components are used. However, a large tank means a very high demand on computational resources. The mesh size from the previous section is not adopted here due to the computational limits. As a compromise, for a mesh size of 0.05 m is used for the multi-directional irregular wave simulation, bearing in mind the possible energy loss due to the mesh resolution. The results of the uni-directional irregular wave simulations indicate that at the mesh size of 0.05 m, the H_s value is reduced to 93.33% of the input value. This percentage is used to correct the simulation results as a simple compensation. With the current setups, there are about 16 million mesh cells in the numerical wave tank. All simulations are run for 10 min. With 1024 cores used on the supercomputer, it takes typically 80 hours to finish a simulation of 600 s. The wave surface elevation near the cylinder at 370s in the simulation with a H_s of 0.06 m is shown in Fig. 14. One can observe a short-crested wave field around the cylinder. The visualisation demonstrates the effectiveness of the code to generate a multi-directional irregular wave field with a wave spectrum as input. The variation of the numerically calculated and normalised significant wave force F_s are shown Fig. 15 and compared to the experimental measurements [1] with the same setup and input waves. It shows that, with constant peak period and increasing significant wave height, the wave force increases almost linearly with the wave steepness in both experimental and numerical results. However, the numerical simulation shows a smaller slope of wave force increase in comparison to what is shown in the experiment. Comparing the normalised

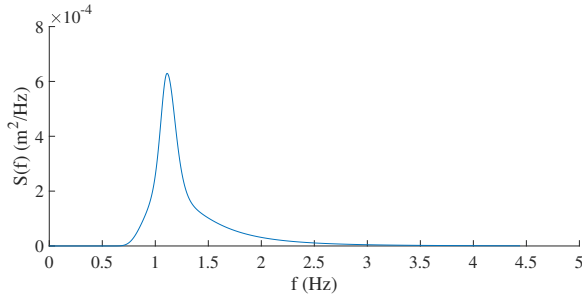


FIGURE 11. The Goda's JONSWAP power spectrum

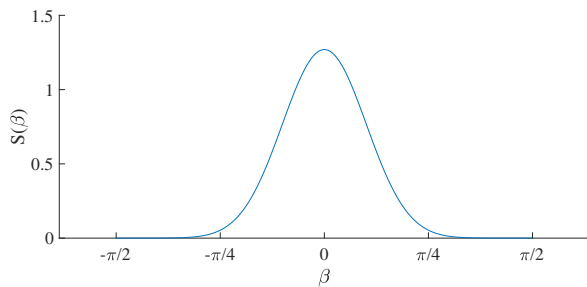


FIGURE 12. The frequency-independent Mitsuyasu directional spreading function

force in Fig. 15 with those in Fig. 10, it is also seen that the wave forces are in general smaller in the multi-directional irregular wave field than in the uni-directional irregular wave field.

The justification for the smaller slope for the change in wave force could be a consequence of a low frequency resolution, which tends to under-represent some larger waves. Therefore, the differences between the different sea states (different wave steepness) are less significant. A thorough study on the sensitivity of multi-directional irregular wave generation to the resolution of frequency and direction components are needed in further study to secure the accuracy of the simulations.

The differences in the wave force values are most probably due to the coarse mesh used in the simulation. A higher mesh resolution means higher demand for computational power and simulation time, especially given the current implementation of the double summation method for the multi-directional irregular wave. The most computational power, approximately 69% of the time consumption for each computational step, is used for the wave generation with the relaxation method. The use of a more efficient wave generation method such as a Dirichlet-type wave generation, an active wave generation method or a better implementation of the double summation method should be investigated in the future.

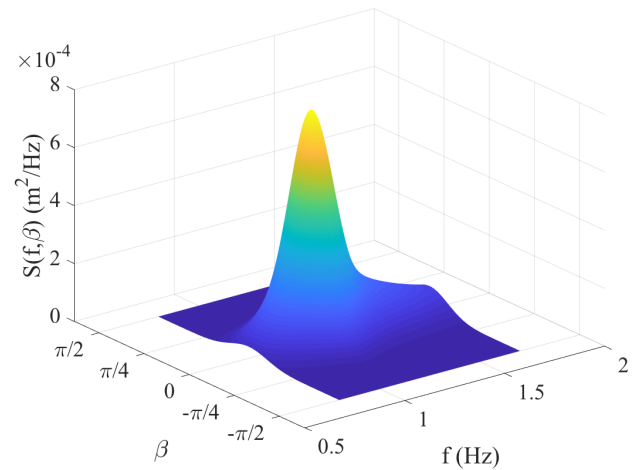


FIGURE 13. The 3D directional spectrum

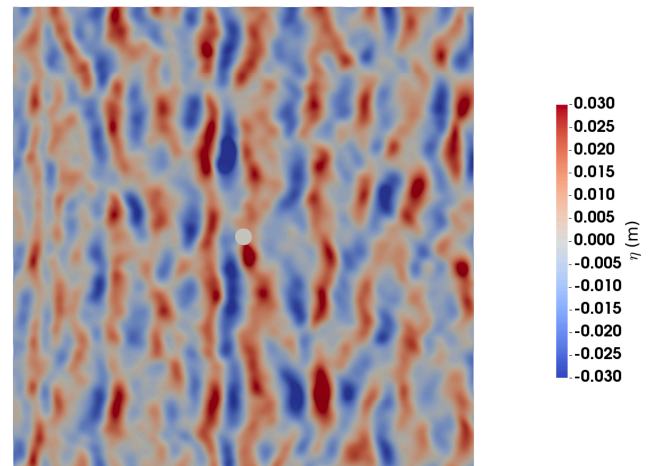


FIGURE 14. The wave surface elevation in the numerical wave tank around the cylinder in the multi-directional irregular wave simulation at $t = 370s$ with $H_s = 0.06m$

CONCLUSIONS

The CFD wave model REEF3D is used to simulate the wave forces on a large cylinder. Regular waves, uni-directional irregular waves and multi-directional irregular waves are simulated with three different steepnesses in each case. The multi-directional irregular wave fields are generated in the CFD numerical tank using input directional wave spectrum. In general, the higher the steepness is, the higher wave forces on the cylinder, and the relation is almost linear. The near-linear scaling also indicates that, with the chosen parameters, the non-linear

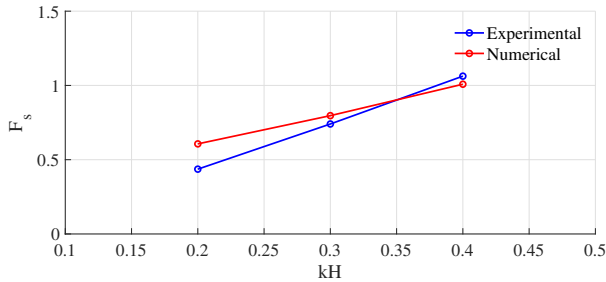


FIGURE 15. The normalised significant wave forces with different steepnesses in the multi-directional irregular wave simulations

effect due to diffraction is not very strong. Future studies will include more non-linearity investigation with different wave parameters. When the irregularity of the wave field increases, especially when the directional spreading effect is increased, the wave force decreases. This further confirms that uni-directional wave simulation tends to overestimate the environmental load in many cases. The multi-directional irregular wave forces on a vertical cylinder in the numerical tank show a similar trend as in the experiment, but with differences in the values and the changing rate. The reasons could be the mesh size, the number of frequency components and the number of direction components in the 3D random wave construction. The sensitivity of all the three factors will be more thoroughly examined in the future. Further, with directional spreading considered, the requirement for computational power increases dramatically, making it hard to apply very fine mesh or a larger number of wave components. A more efficient wave generation method may be developed to replace the current implementation for the multi-directional irregular wave simulations. All the mentioned topics can be explored in the future to improve the accuracy of the model.

In conclusion, a novel method to generate multi-directional irregular waves directly from a directional wave spectrum in a CFD-based numerical wave tank is presented in this paper. The REEF3D wave model demonstrates the ability to carry out such wave generation method but also faces challenges to improve the accuracy. A faster wave generation method and a thorough study of the frequency and angular resolution are needed to further verify and validate the model.

ACKNOWLEDGMENT

This study has been carried out as part of the E39 fjord crossing project (No. 304624) and the authors are grateful for the grants provided by the Norwegian Public Roads Administration. This study was also supported by the computational resources at the Norwegian University of Science and Technology (NTNU) provided by NOTUR, <http://www.notur.no>.

REFERENCES

- [1] Ji, X., Liu, S., Li, J., and Jia, W., 2015. "Experimental investigation of the interaction of multidirectional irregular waves with a large cylinder". *Ocean Engineering*, **93**(Complete), pp. 64–73.
- [2] Morison, J. R., Johnson, J. W., and Schaaf, S. A., 1950. "The force exerted by surface waves on piles". *Journal of Petroleum Technology*, **2**(5), May, pp. 418–423.
- [3] MacCamy, R. C., and Fuchs, R. A., 1954. *Wave forces on piles: a diffraction theory*. Dept. of the Army, Corps of Engineers, Beach Erosion Board, Washington, D.C, USA.
- [4] Kriebel, D., 1990. "Nonlinear wave interaction with a vertical circular cylinder. part i: Diffraction theory". *Ocean Engineering*, **17**(4), pp. 345 – 377.
- [5] Kriebel, D., 1992. "Nonlinear wave interaction with a vertical circular cylinder. part ii: Wave run-up". *Ocean Engineering*, **19**(1), pp. 75 – 99.
- [6] Newman, J. N., 1996. "The second-order wave force on a vertical cylinder". *Journal of Fluid Mechanics*, **320**, p. 417443.
- [7] Wang, C., and Wu, G., 2010. "Interactions between fully nonlinear water waves and cylinder arrays in a wave tank". *Ocean Engineering*, **37**(4), pp. 400 – 417.
- [8] Morgan, G. C. J., and Zang, J., 2010. "Using the RasInterFoam CFD model for non-linear wave interaction with a cylinder". *International Society of Offshore and Polar Engineers*.
- [9] Li, J., Wang, Z., and Liu, S., 2012. "Experimental study of interactions between multi-directional focused wave and vertical circular cylinder, part i: Wave run-up". *Coastal Engineering*, **64**(Supplement C), pp. 151 – 160.
- [10] Li, J., Wang, Z., and Liu, S., 2014. "Experimental study of interactions between multi-directional focused wave and vertical circular cylinder, part ii: Wave force". *Coastal Engineering*, **83**(Supplement C), pp. 233 – 242.
- [11] Ducrozet, G., BONNEFOY, F., Le Touzé, D., and Ferrant, P., 2012. "A modified High-Order Spectral method for wavemaker modeling in a numerical wave tank". *European Journal of Mechanics - B/Fluids*, **34**, July, p. <http://dx.doi.org/10.1016/j.euromechflu.2012.01.017>.
- [12] Ducrozet, G., Bonnefoy, F., Le Touzé, D., and Ferrant, P., 2016. "HOS-ocean: Open-source solver for nonlinear waves in open ocean based on High-Order Spectral method". *Computer Physics Communications*, **203**, June, pp. 245–254.
- [13] Paulsen, B. T., Bredmose, H., and Bingham, H. B., 2014. "An efficient domain decomposition strategy for wave loads on surface piercing circular cylinders". *Coastal Engineering*, **86**, pp. 57 – 76.
- [14] Bihs, H., Alagan Chella, M., Kamath, A., and Arntsen, Ø. A., 2017. "Numerical investigation of focused waves and their interaction with a vertical cylinder using

- REEF3D”. *Journal of Offshore Mechanics and Arctic Engineering*, **139**(4), 05, pp. 041101–041101–8.
- [15] Kamath, A., Alagan Chella, M., Bihs, H., and ivind A. Arntsen, 2015. “Evaluating wave forces on groups of three and nine cylinders using a 3D numerical wave tank”. *Engineering Applications of Computational Fluid Mechanics*, **9**(1), pp. 343–354.
- [16] Kamath, A., Bihs, H., Alagan Chella, M., and ivind A. Arntsen, 2016. “Upstream-cylinder and downstream-cylinder influence on the hydrodynamics of a four-cylinder group”. *Journal of Waterway, Port, Coastal, and Ocean Engineering*, **142**(4), p. 04016002.
- [17] Alagan Chella, M., Bihs, H., Myrhaug, D., and Muskulus, M., 2017. “Breaking solitary waves and breaking wave forces on a vertically mounted slender cylinder over an impermeable sloping seabed”. *Journal of Ocean Engineering and Marine Energy*, **3**(1), pp. 1–19.
- [18] Grotle, E. L., Bihs, H., and sy, V., 2017. “Experimental and numerical investigation of sloshing under roll excitation at shallow liquid depths”. *Ocean Engineering*, **138**(Supplement C), pp. 73 – 85.
- [19] Bihs, H., and Kamath, A., 2017. “A combined level set/ghost cell immersed boundary representation for floating body simulations”. *International Journal for Numerical Methods in Fluids*, **83**(12), pp. 905–916. doi:10.1002/fld.4333.
- [20] Wang, W., Bihs, H., Kamath, A., and Arntsen, Ø., 2017. “Large scale CFD modelling of wave propagation into Mehamn harbour”. *Proceedings of MARINE 2017 Computational Methods in Marine Engineering VII*.
- [21] Wang, W., Bihs, H., Kamath, A., and Arntsen, Ø., 2017. “Large scale CFD modelling of wave propagation in Sulafjord for the E39 project”. *Proceedings of MekIT17 - 9th national conference on Computational Mechanics*.
- [22] Guang-Shan, J., and Chi-Wang, S., 1996. “Efficient implementation of weighted ENO schemes”. *Journal of Computational Physics*, **126**(1), pp. 202–228.
- [23] Shu, C., and Osher, S., 1988. “Efficient implementation of essentially non-oscillatory shock-capturing schemes”. *Journal of Computational Physics*, **77**(2), August, pp. 439–471.
- [24] Falgout, R. D., Jones, J. E., and Yang, U. M., 2006. “Conceptual interfaces in hypre”. *Future Gener. Comput. Syst.*, **22**(1-2), Jan., pp. 239–251.
- [25] Osher, S., and Sethian, J. A., 1988. “Fronts propagating with curvature-dependent speed: Algorithms based on hamilton-jacobi formulations”. *Journal of Computational Physics*, **79**(1), pp. 12 – 49.
- [26] Mayer, S., Garapon, A., and Srensen, L. S., 1998. “A fractional step method for unsteady free-surface flow with applications to non-linear wave dynamics”. *International Journal for Numerical Methods in Fluids*, **28**(2), pp. 293–315.
- [27] Jacobsen, N., Fuhrman, D., and Fredse, J., 2012. “A wave generation toolbox for the open-source CFD library: OpenFoam”. *International Journal for Numerical Methods in Fluids*, **70**(9), pp. 1073–1088.
- [28] Goda, Y., 2000. *Random seas and design of maritime structures*. Advanced Series on Ocean Engineering, World Scientific.
- [29] Mitsuyasu, H., 1975. “Observations of the directional spectrum of ocean waves using a clover-leaf buoy”. *Journal of Physical Oceanography*, pp. 750–760.
- [30] You, Z.-J., 2008. “A close approximation of wave dispersion relation for direct calculation of wavelength in any coastal water depth”. *Applied Ocean Research*, **30**(2), pp. 113 – 119.